

Low-contrast and low-counting-rate measurements in neutron interferometry

H. Rauch, J. Summhammer, and M. Zawisky

Atominstytut der Österreichischen Universitäten, A-1020 Wien, Austria

E. Jericha

Institut für Kernphysik, Technische Universität, A-1040 Wien, Austria

(Received 16 April 1990)

Here we discuss the limits of the recognizability of neutron interference patterns either observed in low-contrast measurements or when collecting very few neutrons only. Low contrast can be caused by a strong beam attenuation or by a large phase shift applied to one beam path. Stochastic and deterministic cases have different influences on the interference pattern, which can be interpreted as a different wavelike or particlelike behavior of the system. Measurements of interference patterns with very few neutrons only are related to the phase-particle-number uncertainty relation, which is discussed on the basis of stochastic and quantum theory arguments. Analogies between coherent-state behavior known in atomic physics and the behavior of neutrons in an interferometer are discussed also.

I. INTRODUCTION

Neutron interferometry has been developed for thermal, cold, and ultracold neutrons.¹⁻⁴ Since its invention it has been used for many fundamental investigations concerning the wave-particle duality and the gravitational, electromagnetic, and strong interaction of the neutron with its surroundings.⁵⁻⁸ Neutrons are massive particles with many well-defined particle properties including an internal quark structure, but they behave in neutron interferometry like waves according to the complementarity principle of quantum mechanics. All the performed experiments belong to the regime of self-interference because the phase-space density of any neutron beam is extremely low (10^{-14}) and in nearly every case when a neutron passes through the interferometer the next neutron is still in a uranium nucleus of the reactor fuel. Therefore, in general, one observes, first-order interference fringes that are caused by a variable phase difference ϕ of two overlapping coherent beams. The degree of coherence is defined as the absolute value of the autocorrelation function of the overlapping beams, which can be determined experimentally from the visibility of the interference fringes^{9,10}

$$I \propto 1 + \langle |\Gamma(\Delta)| / |\Gamma(0)| \rangle \cos\phi$$

with (1)

$$\Gamma(\Delta) = \langle \psi^*(0)\psi(\Delta) \rangle,$$

where Δ is the optical path difference and ϕ the phase difference of the interfering beams ($\phi = \mathbf{k} \cdot \Delta$).

A reduction of the visibility can be caused by a nonuniform phase shift across the beam, by a spatial shift of one wave train relative to the other in the order of the coherence lengths of the beam,¹¹⁻¹³ or by the attenuation of one of the interfering beams.^{14,15} Most interference experiments aim high visibility at high counting rates in or-

der to determine the phase difference as accurately as possible. Contrary to those experiments we are here dealing in the first part with experiments that show a low contrast and in the second part with such ones of very low counting rates. Both kinds are related to the question of the statistical and physical significance of an interference pattern and treat the limiting cases where interference phenomena can still be detected.

II. CONTRAST REDUCTION BY BEAM ATTENUATION

The simplest way for beam attenuation is by inserting an absorbing material into one of the coherent beams of an interferometer. The absorption process can be described by an imaginary part of the index of refraction, yielding a complex phase shift

$$\phi = \phi' + i\phi'' , \quad (2)$$

with $\phi' = -Nb_c\lambda D$ and $\phi'' = N\sigma_t D/2$, where D is the thickness of the sample along the beam path, N is the particle density, b_c is the coherent scattering length of the sample, λ is the wavelength of the neutrons, and $\sigma_t = \sigma_a + \sigma_s$ is the total cross section including absorption and scattering effects in order to fulfill the optical theorem of general diffraction theory.¹⁴ In the absorption process of a neutron a compound nucleus is formed with an excitation energy of about 7 MeV, which decays by α , β , or γ radiation, which can be registered by various detectors. Absorption is an irreversible process caused by the statistical formation of the compound nucleus and can be seen as the essential step for a measuring process and indeed any absorbed neutron causes a signal identifying the beam path the neutron has chosen. The residual interference pattern reads as^{15,16}

$$I = I^n(a\epsilon_1 + \epsilon_2) + \frac{I'}{2} [(a+1) + 2\sqrt{a} \cos\phi'] , \quad (3)$$

where I^n denotes the noninterfering part and I^i the interfering part, and ϵ_i are the relative probabilities of the noninterfering part stemming from beam paths I and II, respectively. The beam attenuation (in beam I) is given by $a = I/I_0 = \exp(-N\sigma_t D)$ and can be measured separately when the second beam is closed completely.

If the beam attenuation in one beam path is achieved by a well-defined (deterministic) reduction of the beam cross section or by a slowly rotating chopper disk with a well-defined open-to-closed ratio, the measured intensity behind the interferometer is the sum of the intensities of the open and closed regions (times):

$$I = I^n(a\epsilon_1 + \epsilon_2) + \frac{I^i}{2}[(a+1) + 2a \cos\phi'] . \quad (4)$$

One notices the differences of the interference pattern in the first (stochastic) and in the second (deterministic) case, although the same number of neutrons are absorbed. The amplitude of the interference pattern varies in the first case as \sqrt{a} , and in the second case proportional to a , which gives, especially for strong beam attenuations ($a \ll 1$), marked differences keeping the interference pattern visible in the stochastic case up to surprisingly high beam attenuations.

Related experiments have been performed with a perfect crystal interferometer and different Gd solutions in a quartz container to obtain sufficiently strong beam attenuations, to reduce any small angle scattering effects, and to avoid large phase shifts which would cause a contrast fading due to coherence effects. The interference patterns have been measured with and without the absorber by rotating an auxiliary Al phase shifter to vary ϕ' . Characteristic results for $a = 0.00495(68)$ are shown in Fig. 1. The interference pattern is clearly visible [$|\Gamma| = 0.0378(42)$], while the probability of finding the particle in the beam path without the absorber is already 99.505(68)%. This demonstrates that an interference amplitude $\sqrt{a}I^i$ is triggered that is considerably larger than the (coherent) beam power of the beam behind the absorber ($aI^i/2$). Indications of an interference modulation can even be obtained if the statistical fluctuations of the nonmodulated part become larger than the interference amplitude, i.e., $[I^n(a\epsilon_1 + \epsilon_2) + I^i(1+a)/2]^{1/2} > \sqrt{a}I^i$. The compilation of previous and new results concerning the amplitude attenuation of the interference pattern due to absorption in one beam path is shown in Fig. 2.

The values at very low transmission probabilities lie slightly below the \sqrt{a} curve, which may be caused by experimental errors or by more fundamental phenomena like the presence of fluctuations of the absorption probability.¹⁷ More detailed experiments are in progress.

If two absorbers with beam attenuation factors a and b are inserted in both beams, the interference pattern has to be written as

$$I = I^n(a\epsilon_1 + b\epsilon_2) + \frac{I^i}{2}[(a+b) + 2\sqrt{ab} \cos\phi'] , \quad (5)$$

which has been proven in the course of scattering length measurements of highly absorbing materials.¹⁸ In the case of equal attenuation ($a = b$) the visibility remains unchanged and the interference amplitude is reduced pro-

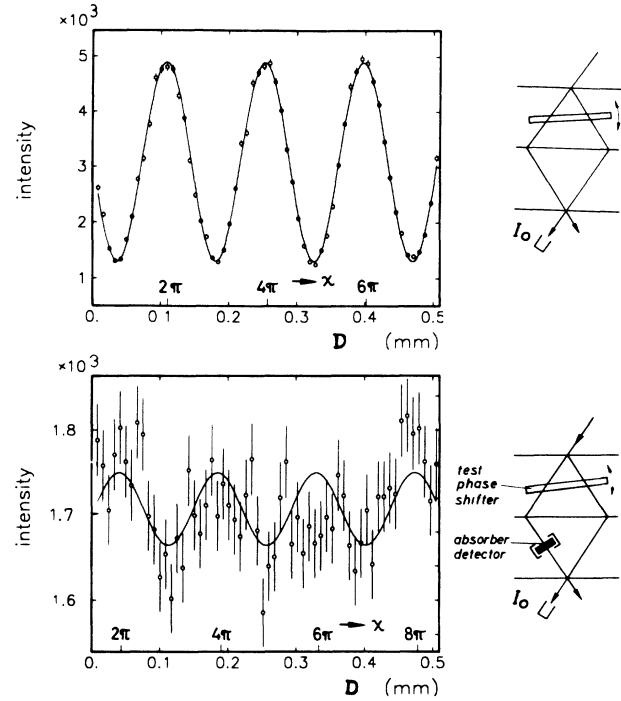


FIG. 1. Interference pattern in forward (0) direction without (above) and with a strong Gd absorber inserted in one beam (below). The intensity values are related to a measuring time of 40 s.

portional to a .

The beams in the interferometer can also be attenuated by coherent or incoherent scattering processes. Related experiments with a perfect silicon crystal placed in a non-dispersive position relative to the interferometer crystal yielded an attenuation factor $a = 0.000325(18)$, which relates to a crystal reflectivity of $R = 0.999675(18)$ and to a fringe visibility of $|\Gamma| = 0.0127(30)$, which is still a measurable signal.¹⁹ This additional coherent beam splitting does not constitute a measurement as the deviated beam can in principle be fed back into the original one. Similar effects occur in the case of diffraction from gratings where a part of the neutrons become labeled neutrons which can be understood as a shift in momentum larger than the widths of the momentum distribution in a certain direction.^{15,19} This changes the autocorrelation function [Eq. (1)] and, therefore, the interference pattern. The reduction of the contrast at high order is caused by the same phenomenon but in spatial coordinates. For Gaussian momentum distribution functions with momentum widths δk the visibility function varies as a function of the phase shift ϕ' as

$$\begin{aligned} \frac{|\Gamma(\Delta)|}{|\Gamma(0)|} &= \exp[-\phi'^2(\delta k/k)^2/2] \\ &= \prod_i \exp[-(\Delta_i \delta k_i)^2/2] , \end{aligned} \quad (6)$$

where it should be mentioned that the momentum resolution δk in perfect crystal interferometry is rather unsymmetric, causing significant differences whether the surface

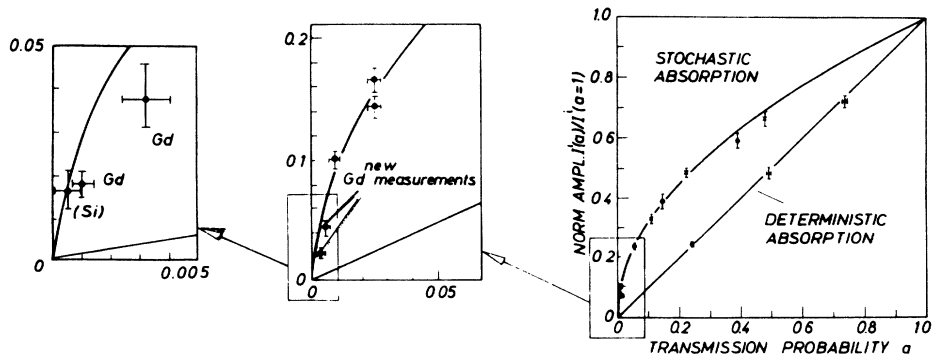


FIG. 2. Normalized interference amplitudes for stochastic and deterministic absorption with special attention for the low transmission case (insets).

of the sample is placed parallel or perpendicular to the reflecting lattice planes of the interferometer crystal.^{13,20} Many related experiments have been reported in the literature.^{11,13} The reduction of the contrast in the neighborhood of the 256th interference order caused by a 35.006(17)-mm-thick Bi phase shifter imposed on a Gaussian beam [$\lambda = 1.9225(24)$ Å] is shown in Fig. 3.¹³ The obvious reduction of the contrast is caused partly by the high-order coherence effect [0.12 from Eq. (6)], the beam attenuation [0.675 from Eq. (3)], and due to the roughness of the surface (0.79). Thus it is partly deterministic and can be undone in the course of the experiment, and partly stochastic, which cannot be undone.

Similar results have been reported for photon experiments where the transmission of the reflecting mirrors was varied.²¹ These measurements were discussed in terms of an unsharp wave-particle behavior^{22,23} or in terms of unsharp measuring procedures, where the term “unsharp” has nothing in common with the term “inaccurate.”²⁴ Various models mainly based on information-theory arguments claim different conservation laws for the particle and wave knowledge.^{23,25,26} None of them can account for all the phenomena discussed before.

Therefore an alternative formulation will be given in Sec. IV.

III. LOW-COUNTING-RATE PHENOMENA

In this case only few neutrons have been counted and the phase difference ϕ between the coherent beams can be obtained with rather large error bars only, which is related to the phase-particle-number uncertainty principle. In a realistic experiment the intensity behind the interferometer is measured at K different positions j of the phase shifter for a certain period of time or monitor counts. Interferometer theory predicts

$$N_j = \bar{N} [1 + V \cos(\phi_j)] \tag{7}$$

and statistical theory yields for an estimate of ϕ_j , if the mean counting rate \bar{N} and the visibility V [$V = \langle |\Gamma(\Delta)| / |\Gamma(0)| \rangle$ of Eq. (1)] are known from other experiments,

$$(\Delta\phi_j)^2 = \frac{N_j}{\bar{N}^2(V^2 - 1) + 2\bar{N}N_j - N_j^2} \tag{8}$$

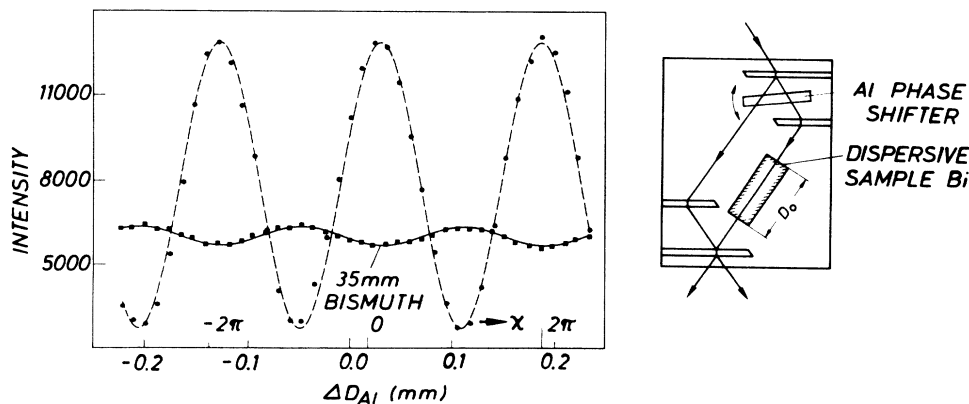


FIG. 3. Interference pattern if a phase shift in the order of the coherence length is applied. The ΔD values belong to the optical path differences caused by the Al auxiliary phase shifter (Ref. 13). The intensity values belong to a measured time of 113 s.

From the K different phase shift settings one obtains an estimate for the phase difference ϕ by χ^2 optimization

$$(\Delta\phi)^2 = \left[\sum_{j=1}^K (\Delta\phi_j)^{-2} \right]^{-1} \quad (9)$$

Approximating the sum by an integral over a definite number of interference fringes one obtains

$$(\Delta\phi)^2 N_t = \left[\frac{fV^2}{2\pi} \int_0^{2\pi} \frac{\sin^2\alpha}{1-f+V(1-2f)\cos\alpha-fV^2\cos^2\alpha} d\alpha \right]^{-1} \xrightarrow{V \rightarrow 1} (1 + \sqrt{1-2f})^{-1} \xrightarrow{f \rightarrow \frac{1}{2}} 1, \quad (11)$$

$$(\Delta\phi)^2 (\Delta N)^2 = \frac{1}{1 - (1-V^2)^{1/2}} \xrightarrow{V \rightarrow 1} 1, \quad (10)$$

where ΔN denotes the standard deviation of the total counting rate N registered at this detector, which obeys Poissonian statistics ($\Delta N = \sqrt{N}$) as a basic feature of the source emission process.

If one includes the counting rates observed by the other detector, or if already in the measurements one uses the constraint $N_j^0 + N_j^H = N^B$ (binomial scan), one obtains

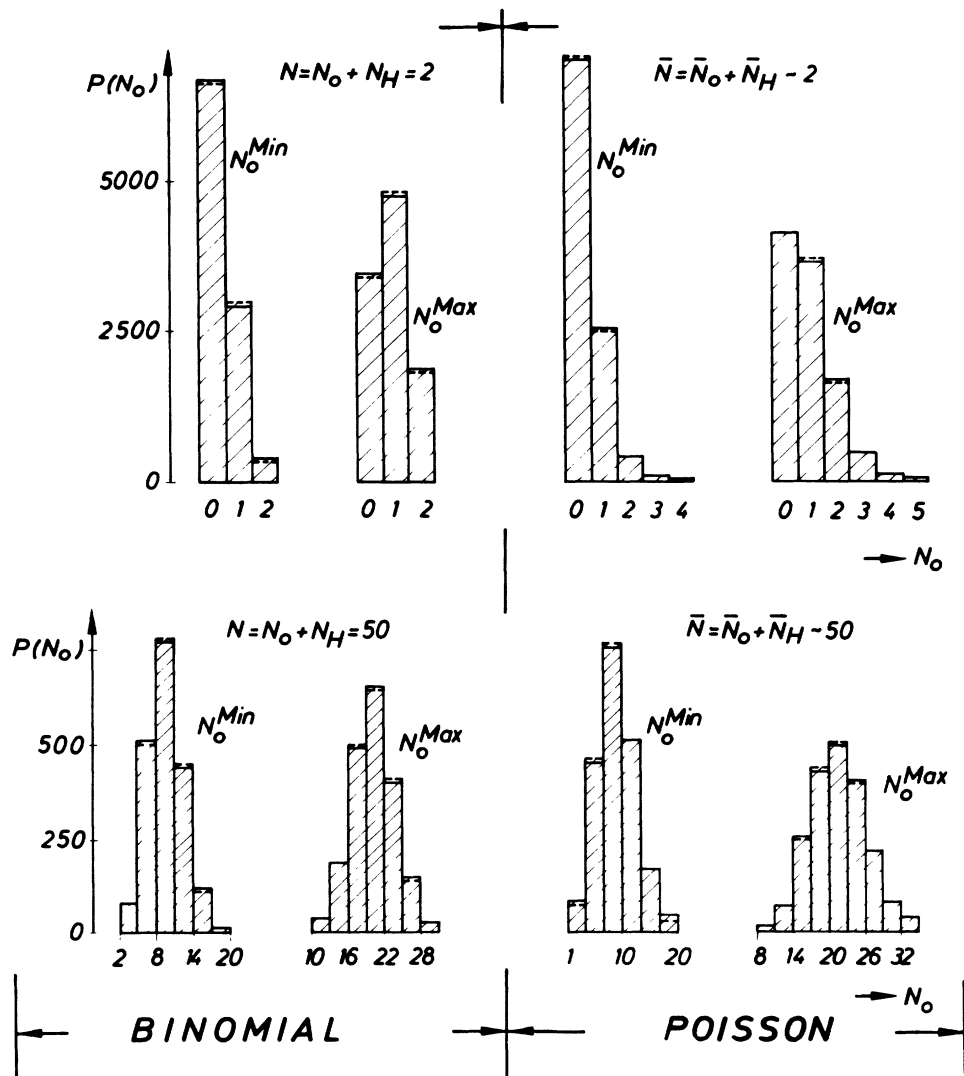


FIG. 4. Measured counting-rate histograms for a binomial (left) and a Poissonian measuring method (right) for very low counting rates ($N \approx 2$, above) and a medium counting rate ($N \approx 50$, below). Each part is divided into a case where there is minimum and maximum counting rate in the 0 detector. Calculated values are shown as dashed lines.

where f is the average fraction of counts the detector in forward direction (0) receives, and $N_t = KN^B$ is the total number of neutrons counted. A comparison of Eq. (10) and (11) shows that using the counts of both detectors increases the accuracy of the phase measurement ideally by a factor of $(N/N_t)^{1/2}$. A similar result has been established by a maximum likelihood analysis.²⁷ A coupling of the interference counting rate to the monitor counting enlarges the uncertainty product up to 1% (for a monitor efficiency of 10^{-4}). Similar results have also been obtained by Yurke²⁸ for an ideal Mach-Zehnder interferometer.

If the visibility is considerably smaller than 1, the term $[1 - (1 - V^2)^{1/2}]^{-1}$ can be approximated by $2/V^2$, which yields for monitor scans

$$(\Delta\phi)^2 N = \frac{2}{V^2}, \tag{12}$$

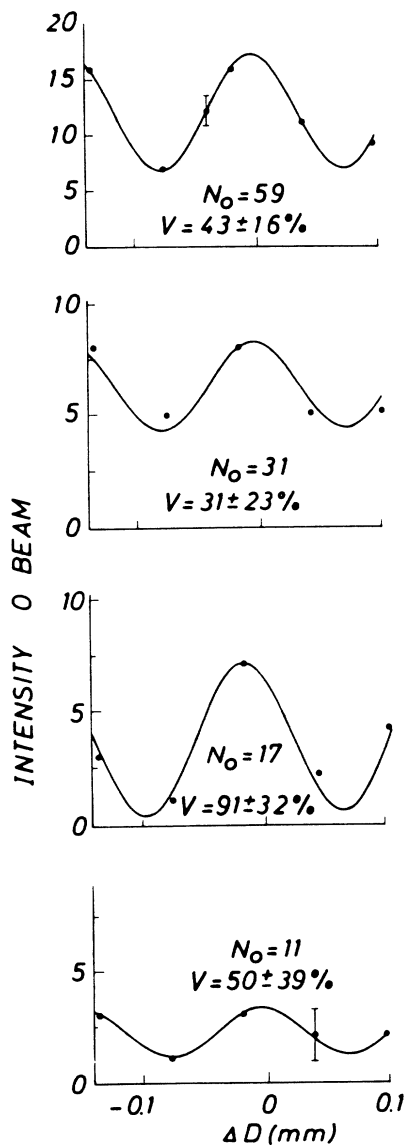


FIG. 5. Characteristic interference pattern taken with rather small numbers of neutrons.

and for binomial scans

$$(\Delta\phi)^2 N_t = \frac{\bar{N}^H}{\bar{N}^0} \frac{2}{V^2}. \tag{13}$$

The difference with the exact formula is of the order of 5% for $V=0.5$.

Related experiments have been performed at the interferometer setup at the 250-kW TRIGA reactor in Vienna, which certainly is an appropriate facility for low-counting-rate phenomena. In the first part of the experiment, histograms were taken of how many counts reach the 0 detector for a fixed monitor counting rate. Many repetitive measurements were done to obtain the distribution function $P(N_j)$, where two positions j were chosen, one at the maximum and one at the minimum intensity in this detector. For both cases a Poisson distribution is expected

$$P(N_j) = \frac{\bar{N}^{N_j}}{N_j!} e^{-\bar{N}}. \tag{14}$$

Analogous measurements with a constant total counting rate yielded binomial statistics ($N^B = N_j^0 + N_j^H$)

$$P(N_j^0) = \frac{N^B!}{N_j^0!(N^B - N_j^0)!} f^{N_j^0} (1-f)^{N^B - N_j^0}. \tag{15}$$

The experimental results show for both cases good agreement with the theoretical predictions (Fig. 4). Whereas in the binomial scans the total number of counts in both detectors is constant, in the monitor scan cases the mean counting rate \bar{N} was chosen to be comparable to that in the related binomial scans.

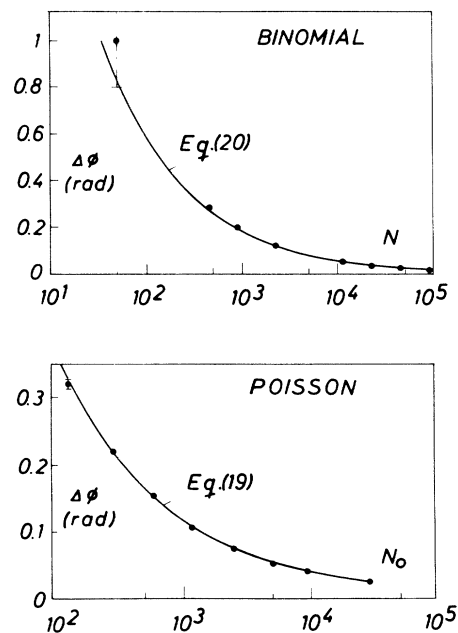


FIG. 6. Measured phase-particle-number uncertainty relation compared to the statistic theory estimate for a binomial (above) and a Poissonian (below) measuring method.

The same setup was used to extract phase information out of fringes measured with only very few neutrons (Fig. 5). These measurements were also repeated many times (up to 10 000 times) and the data points were fitted by means of a least-squares-fit procedure according to Eq. (7). The results obtained are compared to the expected behavior in Fig. 6. The agreement with the predictions of Eqs. (10)–(13) is again fairly good. At the same time these experiments demonstrate the buildup of the interference pattern from single-neutron events as it has been demonstrated in a similar fashion for electron interference patterns.^{29,30}

IV. DISCUSSION

As mentioned in Sec. II the measured reduction of the interference contrast due to absorbing or scattering phase shifters can be visualized as unsharp wave-particle behavior of the system or alternatively to an unsharp measuring procedure.^{22–24} In this respect the behavior of the system changes with increasing absorption from a purely wavelike interference one to a particlelike one with distinct beam path detection.

A measure for the wavelike nature can be found from the correlation function of the interfering beams [Eqs. (1) and (7) with $\bar{N} = I_0 T$, which defines the transparency of the system]

$$W(TV) = TV = \langle |\psi^I \psi^{II}| \rangle, \quad (16)$$

and for the particlelike nature

$$P(TV) = 1 - TV = 1 - \langle |\psi^I \psi^{II}| \rangle, \quad (17)$$

which yields the conservation law

$$P + W = 1, \quad (18)$$

and which describes all the phenomena discussed in Sec. II (Fig. 7). T denotes the general transparency of the system and represents losses which, in principle, are equivalent to having detected a neutron at a certain position in the interferometer, and V is the visibility of the interference pattern. The averages have to be taken over the beam cross section. The different cases are discussed in Ref. 31.

The formulation of the phase–particle-number uncertainty relation in Sec. III is based on standard probability theory and has to be completed in the case of a more rigorous treatment including quantum-mechanical effects.^{32–34} The fermion character of neutrons does not appear directly because the low intensities involved in any kind of neutron interference experiment make particle-particle interaction negligible. In this case Fermi-Dirac statistics approaches Bose statistics because successive neutrons are generally separated in time, space, and momentum.³⁵ Such systems are generally de-

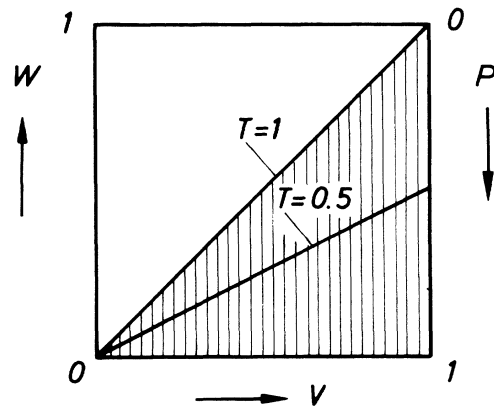


FIG. 7. Synopsis of wavelike and particlelike character of neutrons in different experimental situations.

scribed by coherent states^{35–37} whose associated number states are Poisson distributed and whose phase-difference—particle-number uncertainty relation can be written as^{33,38}

$$(\Delta\phi)^2 = 1 - e^{-N} - N^2 e^{-4N} \left[\sum_{n=0}^{\infty} \frac{N^n}{n! \sqrt{n+1}} \right]^4, \quad (19)$$

which reduces for $N \gg 1$ to the statistical limit discussed before [Eq. (8)], but which deviates from that value for $N \rightarrow 0$ due to projection states onto the vacuum state. Similar behavior has also been verified in the analysis of low-counting-photon experiments.^{33,38}

The analogy between coherent states and free, but coherently coupled, particle motion inside an interferometer addressed here needs further justification. By weakening the harmonic potential, which is generally used to define coherent states, the characteristic level structure disappears and reaches the limiting case of a momentum distribution function which characterizes the free-moving particle beam. The consistency of the coherence lengths, which are determined by the momentum distributions, can be seen as an analog to the uniform wave-packet phenomena in coherent atomic states. Additionally, a time average has to be taken instead of an ensemble average which is equivalent in any ergodic interpretation of quantum mechanics. Thus the coherently split k states (\mathbf{k} and $\mathbf{k} + \mathbf{G}$, where \mathbf{G} is a reciprocal-lattice vector) with a phase difference ϕ exhibit properties similar to coherent-state phenomena.

ACKNOWLEDGEMENTS

The financial support from the Fonds zur Förderung der Wissenschaftlichen Forschung (Project No. S 4201) is gratefully acknowledged.

¹H. Maier-Leibnitz and T. Springer, Z. Phys. **167**, 386 (1962).

²H. Rauch, W. Treimer, and U. Bonse, Phys. Lett. **47A**, 369 (1974).

³A. I. Ioffe, V. S. Zabiyaikin, and G. M. Drabkin, Phys. Lett.

111, 379 (1985).

⁴M. Gruber, K. Eder, A. Zeilinger, R. Gähler, and W. Mampe, Phys. Lett. A **140**, 363 (1989).

⁵Neutron Interferometry, edited by U. Bonse and H. Rauch

- (Clarendon, Oxford, England, 1979).
- ⁶A. G. Klein and S. A. Werner, *Rep. Prog. Phys.* **46**, 259 (1983).
- ⁷H. Rauch, *Contemp. Phys.* **27**, 345 (1986).
- ⁸*Matter Wave Interferometry*, edited by G. Badurek, H. Rauch, and A. Zeilinger, (North-Holland, Amsterdam, 1988).
- ⁹M. Born, and E. Wolf, *Principles of Optics* (Pergamon, Oxford, England, 1975).
- ¹⁰V. F. Sears, *Neutron Optics* (Oxford University Press, Oxford, England, 1989).
- ¹¹H. Rauch, Ref. 5, p. 161.
- ¹²H. Kaiser, S. A. Werner, and E. A. George, *Phys. Rev. Lett.* **50**, 560 (1983).
- ¹³H. Rauch, E. Seidl, D. Tuppinger, D. Petrascheck, and R. Scherm, *Z. Phys. B* **69**, 313 (1987).
- ¹⁴V. F. Sears, *Phys. Rep.* **82**, 1 (1982).
- ¹⁵H. Rauch and J. Summhammer, *Phys. Lett.* **104**, 44 (1984).
- ¹⁶J. Summhammer, H. Rauch, and D. Tuppinger, *Phys. Rev. A* **36**, 4447 (1987).
- ¹⁷N. Namiki and S. Pascazio (private communication).
- ¹⁸H. Rauch and D. Tuppinger, *Z. Phys. A* **322**, 427 (1985).
- ¹⁹H. Rauch, J. Schmiedmayer, M. Zawisky, and E. Jericha (unpublished).
- ²⁰D. Petrascheck, *Phys. Rev. B* **35**, 6549 (1987).
- ²¹P. Mittelstaedt, A. Prior, and R. Schieder, *Found. Phys.* **17**, 891 (1987).
- ²²W. K. Wootters and W. H. Zurek, *Phys. Rev. D* **19**, 473 (1979).
- ²³P. Busch, *Found. Phys.* **17**, 905 (1987).
- ²⁴P. Mittelstaedt, in *Foundations of Quantum Mechanics*, edited by Shun-ichi Kobayashi *et al.* (The Physical Society of Japan, Tokyo, 1990), p. 153.
- ²⁵D. M. Greenberger and H. Yasin, *Phys. Lett. A* **128**, 391 (1988).
- ²⁶A. Zeilinger, *Physica B* **137**, 235 (1986).
- ²⁷G. I. Opat (private communication).
- ²⁸B. Yurke, *Phys. Rev. Lett.* **56**, 1515 (1986).
- ²⁹H. Lichte, in *New Techniques and Ideas in Quantum Measurement Theory*, edited by D. M. Greenberger (Academy of Science, New York, 1988), p. 175.
- ³⁰A. Tonomura, J. Endo, T. Matsuda, and T. Kawasaki, *Am. J. Phys.* **57**, 117 (1989).
- ³¹H. Rauch, in *Foundations of Quantum Mechanics*, edited by Shun-ichi Kobayashi *et al.* (The Physical Society of Japan, Tokyo, 1990), p. 3.
- ³²P. Carruthers and M. M. Nieto, *Phys. Mod. Phys.* **40**, 411 (1968).
- ³³M. M. Nieto, *Phys. Lett.* **60A**, 401 (1977).
- ³⁴D. T. Pegg and S. M. Barnett, *Europhys. Lett.* **6**, 483 (1988).
- ³⁵E. Ledinegg and E. Schachinger, *Phys. Rev. A* **27**, 2555 (1983).
- ³⁶R. J. Glauber, *Phys. Rev. Lett.* **10**, 84 (1963).
- ³⁷E. C. G. Sundarskan, *Phys. Rev. Lett.* **10**, 227 (1963).
- ³⁸H. Gerhardt, H. Welling, and D. Frolich, *Appl. Phys.* **2**, 91 (1973).